Separation Science and Technology
Publication details, including instructions for authors and subscription information:
http://www.informaworld.com/smpp/title~content=t713708471

Extracellular Polymeric Substances in Fouling Layer

Ming-Yuan Chen[a]; Duu-Jong Lee[a]; J. H. Tay[b]
[a] Department of Chemical Engineering, National Taiwan University, Taipei, Taiwan [b] Division of Environmental & Water Resources Engineering, School of Civil & Environmental Engineering, Nanyang Technological University, Singapore

To cite this Article Chen, Ming-Yuan , Lee, Duu-Jong and Tay, J. H.(2006) 'Extracellular Polymeric Substances in Fouling Layer', Separation Science and Technology, 41: 7, 1467 — 1474
To link to this Article: DOI: 10.1080/01496390600683597
URL: http://dx.doi.org/10.1080/01496390600683597

Separation Science and Technology, 41: 1467–1474, 2006

ISSN 0149-6395 print/1520-5754 online
DOI: 10.1080/01496390600683597

Extracellular Polymeric Substances in Fouling Layer

Ming-Yuan Chen and Duu-Jong Lee
Department of Chemical Engineering, National Taiwan University, Taipei, Taiwan

J. H. Tay
Division of Environmental & Water Resources Engineering, School of Civil & Environmental Engineering, Nanyang Technological University, Singapore

Abstract: Membrane biofouling via microbial products limits the feasibility of utilizing membrane bioreactor (MBR) for treating wastewater. Fouling layer would be built up when activated sludge was filtered with a mixed cellulose ester membrane. This study probed the three-dimensional distributions of protein, α-polysaccharide, and β-polysaccharide in fouling layer using fluorescently labeled lectins and fluorescein isothiocyanate (FITC) as staining agents in combination with confocal laser scanning microscopy (CLSM). These extracellular polymeric substances (EPS) distributed heterogeneously in the fouling layer, with α-polysaccharide being concentrated close to the membrane surface. The flow pattern yielded in the fouling layer determines the filtration resistance of biofouling.

Keywords: Fouling layer, extracellular polymeric substances, protein, polysaccharide, CLSM

INTRODUCTION

Membrane fouling results in flux decline and increase in pressure drop across the membrane, thereby producing trouble or even failure of practice (1). The

Received 20 November 2005, Accepted 17 January 2006
Address correspondence to Duu-Jong Lee, Department of Chemical Engineering, National Taiwan University, Taipei 106, Taiwan. Tel.: +886-2-2362-5632; E-mail: djlee@ntu.edu.tw

extracellular polymeric substances (EPS) have been identified as the primary foulants in MBR processes (2–6). The specific resistance of the membrane examined by Rojas et al. (7) increased 10-fold when protein concentrations increased from 30 to 100 mg l^{-1}. Lee et al. (8) indicated that supernatant, at most, contributed 37% of total resistance in membrane filtration. However, Bouhabila et al. (9) found that total resistance of filtration by the supernatant was 76%. Wisniewski and Grasmick (10) attributed roughly 50% of total resistance in filtration to soluble microbial products (SMP) in supernatant. Lee et al. (11) observed that attached cells and the SMPs produced a dynamic membrane.

In biofilm studies, the biofilm was stained and probed using confocal laser scanning microscopy (CLSM) (12–14). Lee et al. (15) probed the bacteria, polysaccharide, and protein in the biofilm using multi-staining with SYBR Green I, fluorescently labeled lectins and Hoechst 2495. This study probed the three-dimensional distributions of protein, α-polysaccharide, and β-polysaccharide in a fouling layer formed during filtration of wastewater sludge staining and CLSM imaging.

EXPERIMENTAL

The Sample

Waste activated sludge was extracted from a wastewater treatment plant of the Presidental Enterprise Corp., Taiwan, which daily treats 250 tons of food-processing wastewater using primary, secondary, and tertiary treatments. The pH of the sludge was about 6.84. The chemical oxygen demand (COD) for the sludge and for filtrate (through 0.45-μm membrane) was 16,000 mg l^{-1} (TCOD) and 86.7 mg l^{-1} (SCOD), respectively, as determined by directly reading a spectrometer (DR/2000, HACH, USA). The elemental composition of the dried samples was C: 41.3%, H: 6.6% and N: 5.4%, according to an elemental analyzer (Perkin-Elmer 2400 CHN).

The supernatant of sludge after 30-min settling was the testing sample. Most flocs were removed to highlight the contribution of colloidal fractions in supernatant to fouling layer formation.

Dead-end membrane filtration tests on collected activated sludge samples were conducted at 30 cm-Hg vacuum using a 0.45-μm mixed cellulose ester membrane (Advantec MFS Inc., CA, USA). Membrane fouling occurred rapidly in the test by noting the declining filtrate flux over the test. The membrane together with the fouling layer was removed from the filtration chamber under fully hydrated condition for further processing.

Staining

Fluorescein isothiocyanate (FITC) (Molecular Probes, Eugene, USA) was used to stain the amine-reactive compounds like protein and amino-sugars.

Fluorescently labelled lectins Concanavalin A (Con A, Molecular Probes, Eugene, USA) conjugated with tetramethylrhodamine were used to bind to α-mannopyranosyl and α-glucopyranosyl sugar residues. Calcofluor white (Sigma) was used to stain the β-linked D-glucopyranose polysaccharides.

In staining, 0.1 M sodium bicarbonate buffer was first added to sample to maintain the amine group in non-protonated form, then the FITC solution ($10\,g\,l^{-1}$) was added to the sample for 1 h at room temperature. Next, the Con A solution ($0.2\,g\,l^{-1}$) was added to the sample, incubated for another 30 min. Afterward, Calcofluor white (Sigma) was used to stain the β-linked D-glucopyranose polysaccharides. After each staining mentioned above, the sample was washed twice to remove extra stain by phosphate buffered saline (PBS).

Some stained membranes were frozen at $-20^{\circ}C$ and cut into specimens of 40-μm thickness using a cryomicrotome for imaging.

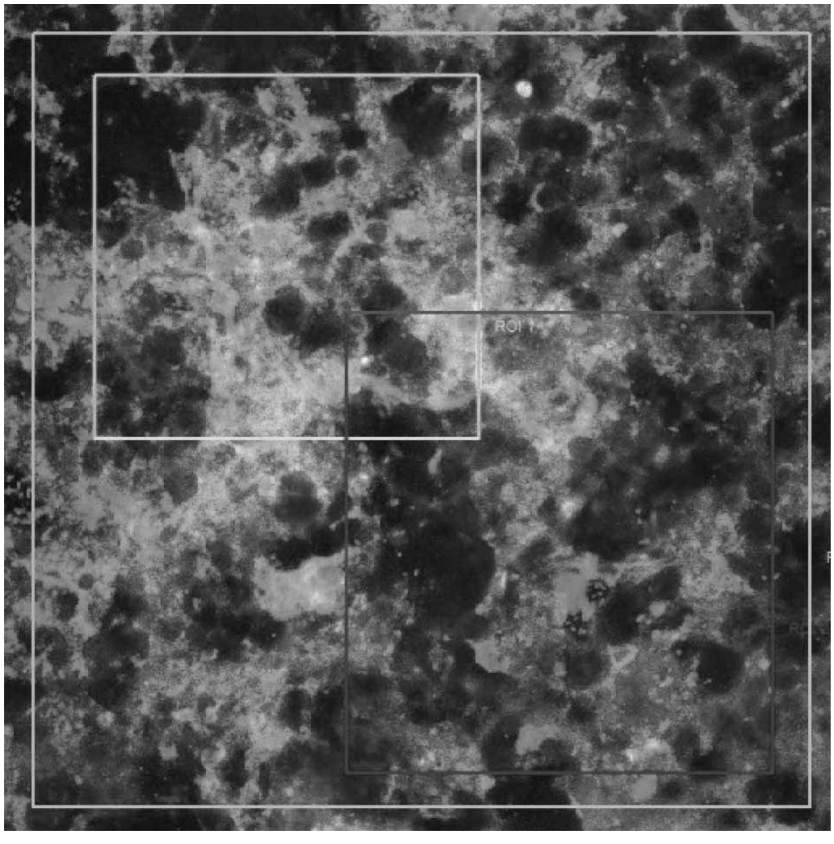

Figure 1. Top view of CLSM image of fouling layer. Green: protein; red: a α-polysaccharide; blue: β-polysaccharide.

CLSM and Image Analysis

To probe the internal structure of the fouling layer, the confocal laser scanning microscopy (CLSM; Leica TCS SP2 Confocal Spectral Microscope Imaging System; TCS SP2) was used. The fouled membrane was imaged from the top surface and from the side (on microtome images) with a 100× objective and analyzed with the Leika confocal software. The FITC probe was detected by excitation with an argon laser at 488 nm and emission 500–540 nm (green). A helium-neon green laser at 543 nm and emission 550-600 nm (red) was used to detect Con A conjugate. The fluorescence of Calcofluor white was detected by excitation at 400 nm and emission width at 410–480 nm (blue).

RESULTS

Figure 1 shows the top view of the reconstructed three-dimensional image for the fouling layer. Large pores existed in the fouling layer, while the distributions of the protein, α- and β-polysaccharides were non-uniform over the top surface of fouling layer.

Figure 2 shows the side view of a CLSM image of microtome of fouling layer. The layer was of a thickness of around 30 μm, but with a clear heterogeneous distribution of EPS distribution. This observation contradicts with common assumption to adopt a one-dimensional fouling model: (filtration resistance) = (pressure drop)/[(filtrate viscosity)(filtrate flux)]. Since some large pores could determine most filtrate flow regardless of how the rest majority of fouling layer behaved, the fouling layer resistance may not correlate with the bulk characteristics of the layer, such as mean porosity.

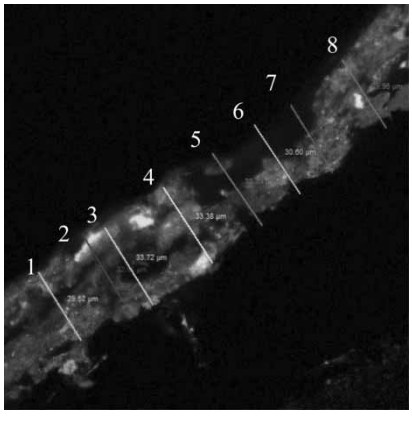

Figure 2. Side view of CLSM image of fouling layer. Green: protein; red: α-polysaccharide; blue: β-polysaccharide. Numerical values in the figure reveal the lines probed the local distributions of EPS.

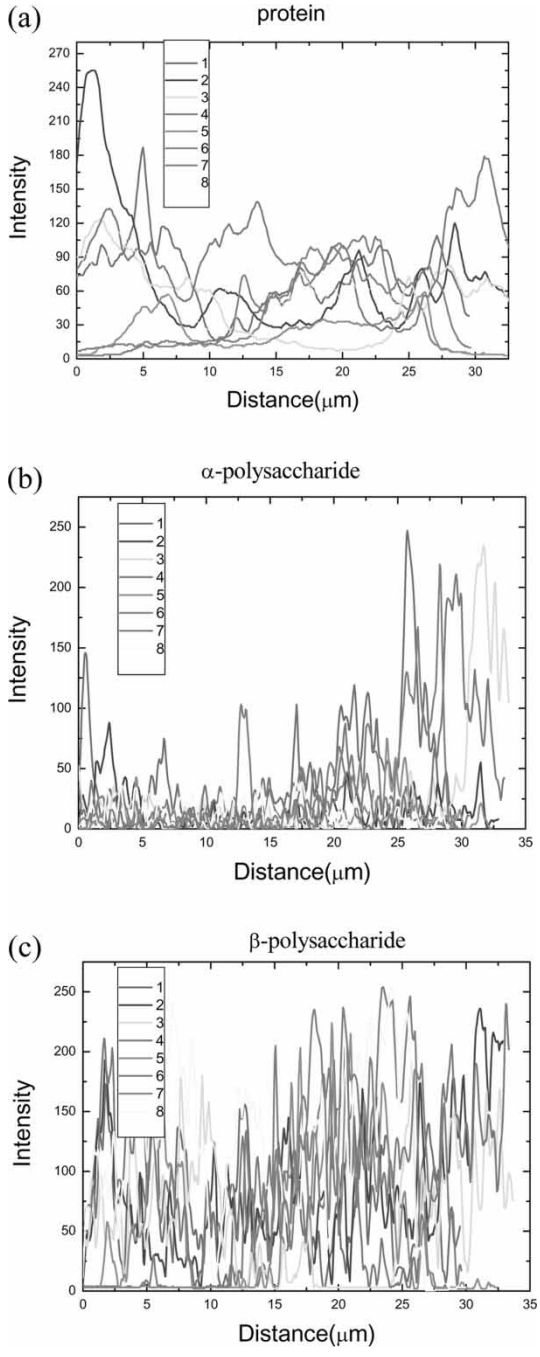

Figure 3. Local distributions of (a) protein; (b) α-polysaccharide; (c) β-polysaccharide. Numerical values reveal the lines shown in Fig. 2.

Figure 3 shows the distributions of the protein, α- and β-polysaccharides along the eight sampling lines demonstrated in Fig. 2. The distribution of EPS in fouling layer is highly stratified. Figure 4 shows the mean and variances of the contents of protein, α-polysaccharide, and β-polysaccharide at the same height from the top of the fouling layer. Although with very large spatial variation, the α-polysaccharide tended to concentrate close to membrane surface, while the protein and the β-polysaccharide were distributed more uniformly across the fouling layer. Moreover, the protein tended to present at the position of high β-polysaccharide content.

Results presented above suggested that the α-polysaccharide presented an important integrant to the initial deposit of the fouling layer. Afterwards, the protein and the β-polysaccharide built up the remaining part of the layer. The detailed structure of the layer determines the filtration resistance induced by biofoluing.

CONCLUSIONS

This study investigated how the main components in excellular polymeric substances (EPS), polysaccharide, and protein, formed a fouling layer on a mixed cellulose ester membrane. Fluorescently labeled lectin Concanavalin A (Con A) and Calcofluor white, and the Fluorescein isothiocyanate (FITC)

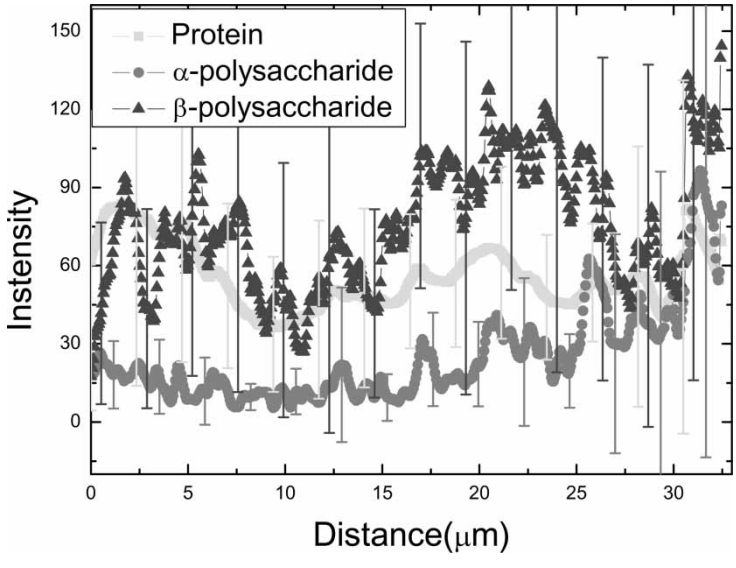

Figure 4. Distributions of protein, α-polysaccharide and β-polysaccharide in fouling layer. Mean and variance were evaluated at the same height from top surface of fouling layer.

were used in combination with confocal laser scanning microscopy to quantitatively describe the compositional distributions of α-polysaccharide, β-polysaccharide, and protein in the formed fouling layer.

The fouling layer consisted of some large pores which could allow easy filtrate flow, thus low filtration resistance over the majority of layer body. The side view of fouling layer revealed a heterogeneous distribution of EPS. Hence, the commonly adopted one-dimensional description to fouling resistance may not be able to correlate with the bulk characteristics of the fouling layer. The EPS distributed in fouling layer in a stratified manner. The α-polysaccharide tended to concentrate close to the membrane surface; while the protein and the β-polysaccharide tended to appear together and distributed relatively more uniformly across the fouling layer. The α-polysaccharide presented an important integrant in initial deposit of fouling layer.

REFERENCES

1. Ramesh, A., Lee, D.J., Wang, M.L., Hsu, J.P., et al. (2006) Biofouling in membrane bioreactor. *Separ. Sci. Technol.*, appeared in this volume.
2. Kimura, K., Yamato, N., Yamamura, H., and Watanabe, Y. (2005) Membrane fouling in pilot-scale membrane bioreactos (MBR2) treating municipal wastewater. *Envir. Sci. Technol.*, 39: 6293–6299.
3. Nagaoka, H., Yamanishi, S., and Miya, A. (1998) Modeling of biofouling by extracellular polymers in a membrane separation activated sludge system. *Water Sci. Technol.*, 38 (4–5): 497–504.
4. Nagaoka, H., Ueda, S., and Miya, A. (1996) Influence of bacterial extracellular polymers on the membrane separation activated sludge process. *Water Sci. Technol.*, 34 (9): 165–172.
5. Leslie, G.L., Schneider, R.P., Fane, A.G., Marshall, K.C., and Fell, C.J.D. (1993) Fouling of a microfiltration membrane by two Gram-negative bacteria. *Colloids Surf. A*, 73: 165–178.
6. Geesey, G.G., Stupy, M.W., and Bremer, P.J. (1992) The dynamics of biofilms. *Int. Biodeterioration Biodegradation*, 30: 135–154.
7. Rojas, M.E.H., Van Kaam, R., Schetrite, S., and Albasim, C. (2005) Role and variations of supernatant compounds in submerged membrane bioreactor fouling. *Desalination*, 179: 95–107.
8. Lee, W., Kang, S., and Shin, H.S. (2003) Sludge characteristics and their contribution to microfiltration in submerged membrane bioreactors. *J. Mem. Sci.*, 216: 217–227.
9. Bouhabila, E.H., Ben Aim, R., and Buisson, H. (2001) Fouling characterization in membrane bioreactors. *Separ. Purif. Technol.*, 22–23, 123–132.
10. Wisniewski, C. and Grasmick, A. (1998) Floc size distribution in a membrane bioreactor and consequences for membrane fouling. *Colloids Surf. A*, 138: 403–411.
11. Lee, J.M., Ahn, W.Y., and Lee, C.H. (2001) Comparison of the filtration characteristics between attached and suspended growth microorganisms in submerged membrane bioreactor. *Water Res.*, 35: 2435–2445.

12. Neu, T.R. and Lawrence, J.R. (1999) Lectin-binding analysis in biofilm system. *Method Enzymol.*, 310: 145–152.
13. Strathmann, M., Wingender, J., and Flemming, H.-C. (2002) Application of fluorescently labeled lectins for the visualization and biochemical characterization of polysaccharides in biofilms of *Pseudomonas Aeruginosa*. *J. Microbiol. Methods,*, 50: 237–248.
14. Yun, M.A., Yeon, K.M., Park, J.S., Lee, C.H., Chun, J., and Lim, D.J. (2006) Characterization of biofilm structure and its effect on membrane permeability in MBR for dye wastewater treatment. *Water Res.*, 40: 45–52.
15. Kim, H.Y., Yeon, K.M., Lee, C.H., Lee, S.H., and Swaminathan, T. (2006) Biofilm structure and extracellular polymeric substances in low and high oxygen bioreactors. *Separ. Sci. Technol.*, appeared in this volume.